2024 IEEE International Conference on Robotics and Automation (ICRA 2024)
May 13-17, 2024. Yokohama, Japan

Energy-Aware Ergodic Search: Continuous Exploration for Multi-Agent Systems with Battery Constraints

Adam Seewald, Cameron J. Lerch, Marvin Chancán, Aaron M. Dollar, and Ian Abraham

***Abstract*—Continuous exploration without interruption is important in scenarios such as search and rescue and precision agriculture, where consistent presence is needed to detect events over large areas. Ergodic search already derives continuous trajectories in these scenarios so that a robot spends more time in areas with high information density. However, existing literature on ergodic search does not consider the robot's energy constraints, limiting how long a robot can explore. In fact, if the robots are battery-powered, it is physically not possible to continuously explore on a single battery charge. Our paper tackles this challenge, integrating ergodic search methods with energy-aware coverage. We trade off battery usage and coverage quality, maintaining uninterrupted exploration by at least one agent. Our approach derives an abstract battery model for future state-of-charge estimation and extends canonical ergodic search to ergodic search under battery constraints. Empirical data from simulations and real-world experiments demonstrate the effectiveness of our energy-aware ergodic search, which ensures continuous exploration and guarantees spatial coverage.**

I. Introduction

Robotic exploration is a recurring problem in different scenarios, e.g., inspection, surveying, etc. It typically involves coverage path planning (CPP), which deals with deriving robots' trajectories that traverse every point in a given space [1–3]. Within CPP, ergodic search is a recent and promising direction [4–17], as it enhances the efficiency of traditional CPP by optimizing the time a robot spends in a given region w.r.t. an information measure. As a result, ergodic search derives trajectories so that the robots spend more time in areas with high information density while quickly passing areas with low information density [13, 18]. The user can specify areas of interest, e.g., where the robots should spend more time exploring in a search and rescue scenario [14], where the robots should collect more data in a precision agriculture scenario [16], etc.

Canonical ergodic search already derives continuous exploration trajectories [5, 15, 19], but it is physically not possible for robots to continue exploring on a single battery charge. Scenarios involving CPP, however, often require that the space is covered continuously. This work enhances the current ergodic search literature by incorporating more traditional energy-aware CPP approaches [20–25], battery- and energy-aware planning [26–29], and planning of energy trade-offs [30, 31]. It answers the question: *Is it possible to tradeoff battery and coverage quality so that there is at least one agent exploring at all times*?

This work was partly supported by Yale University and a gift from the Boston Dynamics AI Institute.

A. S., C. J. L., M. C., A. M. D., and I. A. are with the Department of Mechanical Engineering and Materials Science, Yale University, CT, USA. Email: adam.seewald@yale.edu;

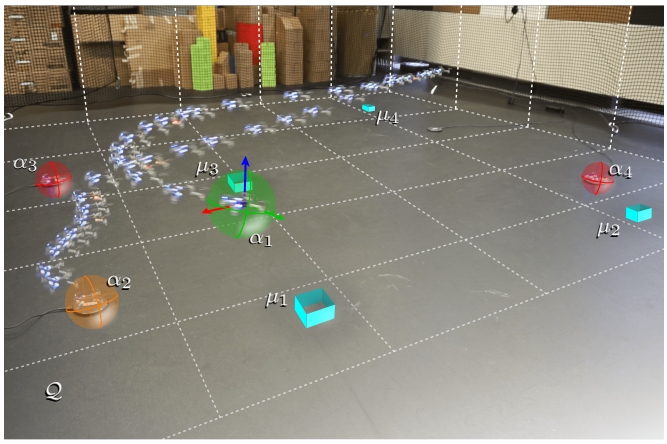

Fig. 1: **Example of energy-aware ergodic search**. A set of agents explores $\mathcal{Q}$, focusing on areas with high information density μ_1, μ_2, μ_3, and μ_4, employing ergodic search. The exploration is continuous and uninterrupted so that there is always one agent exploring – α_1, whereas α_2, α_3, and α_4 are recharging. The colors of the spheres indicate the state of charge.

Prior literature has studied ergodic search in manipulation [8], tactile sensing [15], stochastic dynamics [7, 17], distributed information [5], time optimality [14], and active learning [4]. Ergodic search for multi-agent systems [9, 10] has been applied in conjunction with low-information sensors [10–12], swarms control [9], obstacle avoidance [11], and decentralized systems [12]. Ergodic search has been proven successful in use cases involving urban environments [13] and information gathering [6]. While prior literature includes ergodic search methods in a variety of settings, energy constraints have not been studied yet. Partly due to these constraints, the uninterrupted exploration that considers a spatial distribution is currently hindered.

Our approach derives an abstract battery model [32] for battery state of charge (SoC) estimation at future time instances. We first adapt canonical ergodic search to multi-agent ergodic search [9, 10]. We then utilize the formulation to propose energy-aware ergodic search, i.e., ergodic search under battery constraints. The exploration is continuous and uninterrupted, employing a finite horizon framework reminiscent of a model predictive controller [29]. Experimental data from simulations and real-world experiments show our newly proposed energy-aware ergodic search. We show with empirical evidence that we can effectively explore a space, there is at least one agent exploring, the spatial distribution is satisfied, and the exploration is uninterrupted in Section IV. Figure 1 shows our experimental setup, which resembles a search and rescue scenario. Four agents explore the space where the high information density is represented by cyan boxes. Some agents are actively exploring (green sphere),

while others are grounded and recharging (red and orange spheres). The detailed results from the experimental evaluation and the code to replicate our approach are made available on the project repository webpage[1].

The remainder of the paper is then structured as follows. Sec. II formulates the problem of energy-aware ergodic search. Sec. III discusses the methods for both the canonical ergodic search and our battery model enhanced ergodic search. Sec. V concludes and proposes future directions.

II. Problem Formulation

This work addresses the problem of exploring a bounded space with multiple agents, proportionally to a spatial distribution and in such a way that there is at least one agent exploring. In the remainder of the text, we will use the terms *continuously* and *uninterruptedly* to indicate that there is at least one agent exploring the space at all times, i.e., a certain measurable level of coverage is always satisfied. Canonical ergodic search [4–8, 18, 19] does not deal with uninterrupted exploration. It derives an agent's control – or analogously multiple agents' control [9–13] – so that its trajectory maximizes an ergodic metric in the spectral domain. Let us thus define the concepts of ergodicity and ergodic metric.

Definition II.1 (Ergodicity)**.** Consider a bounded space $\mathcal{Q} \subset \mathbb{R}^D$ of dimension $D \in \mathbb{N}_{>0}$. A trajectory $\mathbf{q}(t) \in \mathcal{Q}$ is *ergodic* with respect to a spatial distribution ϕ, i.e., is distributed among regions of high expected distribution [5], if and only if

$$\lim_{t\to\infty} \frac{1}{t} \int_{\mathcal{T}} \Omega\Big(\kappa\big(\mathbf{q}(t)\big)\Big) = \int_{\mathcal{Q}} \phi(\mathbf{q})\, \Omega(\mathbf{q})\, d\mathbf{q}, \tag{1}$$

for all Lebesgue functions Ω [18]. Here, the function κ maps the state to the exploration workspace.

Definition II.2 (Ergodic metric)**.** Consider a time average distribution that describes where the robot spends more time over a finite time window $[t_0, t_f]$, i.e., $h\big(\mathbf{q}(t)\big) = \int_{\mathcal{T}} \Delta\big(\mathbf{q}(t)\big)\, dt\, /(t_f - t_0)$, Δ is a Dirac delta function, and $t_0, t_f \in \mathbb{R}_{>0}$ are the initial and final time instants. An *ergodic metric* is defined as the L^2 inner product between the time average distribution h and the average of the spatial distribution ϕ.

Problem II.1 (Ergodic search)**.** Consider the bounded space $\mathcal{Q}$ and a spatial distribution ϕ s.t. $\int_{\mathcal{Q}} \phi\, d\mathbf{q} = 1$, $\phi(\mathbf{q}) \geq 0$, $\forall \mathbf{q} \in \mathcal{Q}$. *Ergodic search problem* is the problem of deriving a control action $\mathbf{u}(t) \in \mathcal{U} \subset \mathbb{R}^V$ with $V \in \mathbb{N}_{>0}$ so that the ergodic metric is minimized (see Definition II.2).

We derive an ergodic metric in Equation (3) in Sec. III-A. The notation $\mathbb{R}$ and $\mathbb{N}$ indicates reals and naturals, $\mathbb{N}_{>0}$ strictly naturals. Bold notation is used for vectors.

Let us extend the canonical ergodic search problem to energy-aware ergodic search, i.e., uninterrupted multi-agent exploration under spatial distribution and battery constraints.

Problem II.2 (Energy-aware ergodic search)**.** Consider a set of n agents $\boldsymbol{\alpha} := \{\alpha_1, \alpha_2, \ldots, \alpha_n\}$, a bounded space $\mathcal{Q}$, and a spatial distribution ϕ similar to Problem II.1. *Energy-aware ergodic search problem* is the problem of deriving each agent's ${}^j\alpha$ control action ${}^j\mathbf{u}(t)$ so that $\forall j$, ${}^j\mathbf{q}(t)$ induces a time average distribution $h\big(\mathbf{q}(t)\big)$ that is proportional to the spatial distribution ϕ and the ergodic metric (calculated between the agents' averaged time average distribution in Definition II.2) is satisfied, i.e., there is an upper bound on the ergodic metric for a given $\gamma \in \mathbb{R}_{>0}$.

We will provide a solution to Problem II.2 (see Sec. III), assuming that there are one or more areas in $\mathcal{Q}$ – namely, charging stations – where the agents can land and recharge the battery, using, e.g., wireless charging (see Sec. IV).

III. Methods

In this section, we discuss the methods utilized in this work for continuous, uninterrupted exploration with multiple agents and proportionally to a spatial distribution. We discuss how to achieve the latter in Sec. III-A and the former in Sec. III-B.

A. Ergodic search

To derive an agent's trajectory proportionally to a spatial distribution, canonical ergodic search first requires defining the distribution ϕ. For this purpose, in both Problem II.1 and II.2, let us consider a Gaussian mixture model (GMM)

$$\phi(\boldsymbol{\delta}, \mathbf{q}) := \sum_{k=1}^{m} \delta_k\, \mathcal{N}(\mathbf{q} \,|\, \mu_k, \Sigma_k), \tag{2}$$

composed of m Gaussians $\mathcal{N}$. Each has a covariance matrix $\Sigma_k \in \mathbb{R}^{D\times D}$, center $\mu_k \in \mathcal{Q}$, and positive mixing coefficient $\delta_k \in \boldsymbol{\delta}$ such that, for each k, the sum of δ_k is ≤ 1.

The goal of ergodic search is to minimize an ergodic metric (see Definition II.2) such as [18]

$$\mathcal{E}(\boldsymbol{\delta}, \mathbf{q}(t)) := \frac{1}{2} \sum_{k\in\mathcal{K}} \Lambda_k \big(c_k(\mathbf{q}(t)) - \phi_k(\boldsymbol{\delta})\big)^2, \tag{3}$$

where ϕ_k are coefficients derived utilizing the Fourier series on the spatial distribution ϕ and c_k on the trajectory $\mathbf{q}(t)$. They are detailed in Eq. (7) and (5) respectively. An agent whose trajectory minimizes Eq. (3) for $t \to \infty$ is *optimally ergodic* w.r.t. ϕ [12].

Λ_k is a weight factor. That is, if

$$\Lambda_k = (1 + \|k\|^2)^{(-D-1)/2}, \tag{4}$$

lower frequencies have more weight [5]. $\mathcal{K} \in \mathbb{N}^D$ is a set of index vectors that covers $[K] \times \cdots \times [K] \in \mathbb{N}^{K^D}$ where K is a given number of frequencies with the fundamental frequency [33]. The notation $[K]$ indicates positive naturals up to K.

The coefficients c_k are derived using the Fourier series basis function. If we consider the trigonometric form, they can be expressed

$$c_k(\mathbf{q}(t)) := \int_{\mathcal{T}} \frac{1}{L^D} \prod_{d\in[D]_{>0}} \big(\cos(k_d\, \mathbf{q}_d(\tau)\, \psi) - i \sin(k_d\, \mathbf{q}_d(\tau)\, \psi)\big)\, d\tau / t, \tag{5}$$

[1] github.com/adamseew/enerergo

where ψ is $2\pi/L$ for a given period $L \in \mathbb{R}_{>0}$, i is the imaginary unit, k_d is the dth item of k, and $\mathbf{q}_d$ is the dth item of $\mathbf{q}$.

The interval $\mathcal{T}$ is built so that the integration is between $\tau = t_0$ and t, and the notation $[D]_{>0}$ indicates strictly positive naturals up to D.

To derive the coefficients ϕ_k, let us consider the GMM model in Eq. (2) on a search space $\mathcal{Q}$. The space is further bounded to a symmetric set $[-L/2, L/2]^D$ since the Gaussians are symmetric about the zero axes. As a result, the model can be expressed [33]

$$\Phi(\boldsymbol{\delta}, \mathbf{q}) := \sum_{d \in [2^D]_{>0}} \sum_{k=1}^{m} \delta_k \mathcal{N}(\mathbf{q} \,|\, A_d \mu_k, A_d \Sigma_k A_d^T)/2^D, \quad (6)$$

where $A_d \in \mathbb{R}^{D \times D}$ are linear transformation matrices.

Let us call the integrand in Eq. (5) c. It maps the space to the spectral domain. The equivalent of Eq. (5) for the spatial distribution can be then expressed

$$\phi_k(\boldsymbol{\delta}) := \int_{\mathcal{Q}} \Phi(\boldsymbol{\delta}, \mathbf{q})\, c(\mathbf{q})\; d\mathbf{q}. \quad (7)$$

The space $\mathcal{Q}$ is built so that the integration is within the points of the bounded symmetric set $\mathbf{q} \in [-L/2, L/2]^D$.

Both the coefficients c_k and ϕ_k are evaluated per each k in $\mathcal{K}$ in Eq. (3).

Let us first formulate the solution to Problem II.1, utilizing a formulation borrowed from canonical ergodic search. If the agent's dynamics is described by a generic differential equation $\dot{\mathbf{q}}(t) = f\big(\mathbf{q}(t),\, \mathbf{u}(t)\big)$, an optimal control problem (OCP) that selects an ergodic control can be formulated [17]

$$\min_{\mathbf{q}(t), \mathbf{u}(t)} \int_{\mathcal{T}} \mathbf{u}(\tau)^T R \mathbf{u}(\tau)\, d\tau + \mathcal{E}(\boldsymbol{\delta}, \mathbf{q}(t)), \quad (8a)$$

$$\text{s.t. } \dot{\mathbf{q}} = f(\mathbf{q}(t), \mathbf{u}(t)), \quad (8b)$$

$$\mathbf{q}(t) \in \mathcal{Q},\ \mathbf{u}(t) \in \mathcal{U}, \quad (8c)$$

$$\mathbf{q}(t_0), \mathbf{q}(t_f) \text{ are given}, \quad (8d)$$

where the ergodic metric is derived in Eq. (3), $R \in \mathbb{R}^{V \times V}$ is a control penalizing diagonal positive-definite matrix, and t_0, t_f are the first and last time instants respectively. The interval $\mathcal{T}$ is $[t_0, t_f]$.

To formulate the solution to Problem II.2, let us first extend the OCP in Eq. (8) to multi-agent systems. Eq. (8a) becomes

$$\min_{\boldsymbol{\Theta}} \; \frac{1}{n} \left(\sum_{k=1}^{n} \int_{\mathcal{T}_k} {}^k\mathbf{u}(\tau)^T R_k\, {}^k\mathbf{u}(\tau)\, d\tau \right) + \mathcal{E}(\boldsymbol{\delta}, \boldsymbol{\Theta}_\mathbf{q}), \quad (9)$$

where the control penalizing term R_k is now agent-specific. The term $\boldsymbol{\Theta}_\mathbf{q}$ is ${}^1\mathbf{q}(t), {}^2\mathbf{q}(t), \ldots, {}^n\mathbf{q}(t)$, and $\boldsymbol{\Theta}$ is $\boldsymbol{\Theta}_\mathbf{q}, {}^1\mathbf{u}(t), {}^2\mathbf{u}(t), \ldots {}^n\mathbf{u}(t)$. $\mathcal{T}_k$ is $[{}^kt_0, {}^kt_f]$, i.e., different agents might have different durations.

The ergodic metric is now evaluated for multiple agents

$$\mathcal{E}(\boldsymbol{\delta}, \boldsymbol{\Theta}_\mathbf{q}) := \frac{1}{2} \sum_{k \in \mathcal{K}} \Lambda_k \left(\frac{1}{n} \sum_{j \in [n]} c_k({}^j\mathbf{q}(t)) - \phi_k(\boldsymbol{\delta}) \right)^2. \quad (10)$$

Let us consider a vector $\mathbf{b} \in \mathbb{R}^3$, detailed later in Sec. III-B, whose trajectory $\mathbf{b}(t)$ describes the evolution of some battery metrics' in time. If $\mathbf{b}_{\text{SoC}}$ is the value of the vector that expresses the battery SoC, the expression in Eq. (9) might select ergodic metrics corresponding to trajectories that are impossible to traverse in the $\mathbf{b}_{\text{SoC}} \in (0, 1]$ domain. In order to satisfy the battery SoC domain and always keep at least one agent exploring, an OCP must satisfy an additional constraint

$$\exists k \in [n] \text{ s.t. } {}^k\mathbf{b}_{\text{SoC}}(t_f) \in (0, b_f], \quad (11)$$

where $b_f \in (0, 1] \subset \mathbb{R}_{>0}$ is a given desired battery SoC at the final time instant.

Finally, let us consider the realistic assumption that the optimization horizon is known and is, e.g., an empirically collected value that corresponds to one of the agents' discharge times (see Sec. IV).

The OCP that provides a solution to Problem II.2 can be formulated

$$\min_{\boldsymbol{\Theta}} \; \frac{1}{n} \sum_{k=1}^{n} \int_{\mathcal{T}_k} {}^k\mathbf{u}(\tau)^T R_k\, {}^k\mathbf{u}(\tau)\, d\tau, \quad (12a)$$

$$\text{s.t. } {}^1\dot{\mathbf{q}}(t) = f_1({}^1\mathbf{q}(t), {}^1\mathbf{u}(t)), \ldots, {}^n\dot{\mathbf{q}}(t) = f_n({}^n\mathbf{q}(t), {}^n\mathbf{u}(t)), \quad (12b)$$

$${}^1\mathbf{q}(t), \ldots, {}^n\mathbf{q}(t) \in \mathcal{Q},\ {}^1\mathbf{u}(t), \ldots, {}^n\mathbf{u}(t) \in \mathcal{U}, \quad (12c)$$

$$\exists k \in [n] \text{ s.t. } {}^k\mathbf{b}_{\text{SoC}}(t_f) \in (0, b_f], \quad (12d)$$

$$\mathcal{E}(\boldsymbol{\delta}, \boldsymbol{\Theta}_\mathbf{q}) \leq \gamma, \quad (12e)$$

$$g_1(\boldsymbol{\delta}, {}^1\mathbf{q}(t), {}^1\mathbf{u}(t)) \leq 0, \ldots, g_n(\boldsymbol{\delta}, {}^n\mathbf{q}(t), {}^n\mathbf{u}(t)) \leq 0, \quad (12f)$$

$${}^1\mathbf{q}(t_0), {}^1\mathbf{q}(t_f), \ldots, {}^n\mathbf{q}(t_0), {}^n\mathbf{q}(t_f), b_f, \gamma \text{ are given}, \quad (12g)$$

where constraints in Eq. (12f) are optional and express additional requirements (see Sec. IV). The constraint in Eq. (12d) ensures that there is at least one agent exploring at all time instants in the optimization horizon. The ergodic metric is integrated into the constraint as proposed in [14], and the evolutions of the agents' states in time are described by generic differential equations ${}^k\dot{\mathbf{q}}(t) = f_k({}^k\mathbf{q}(t), {}^k\mathbf{u}(t))$.

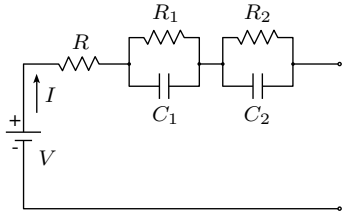

Fig. 2: **Abstract equivalent circuit model** for state-of-charge estimation [34]. The model consists of a second-order resistor-capacitor circuit with two resistors R_1 and R_2 and two capacitors C_1 and C_2 in two separate circuit elements. An additional resistor R is also employed.

B. Battery modeling

To derive a battery model for continuous exploration – a model that allows us to predict when an agent is exploring and when it conversely should be recharging the battery – let us consider an abstract equivalent circuit model (ECM). These models are commonly employed in battery metrics estimation for robots and other applications, especially if equipped with rechargeable battery cells [29, 35–39].

The ECM model we employ is a second-order resistor-capacitor (RC) circuit model, as illustrated in Fig. 2 [34]. Formally, it can be expressed [32]

$$\dot{\mathbf{b}}(t) = \begin{bmatrix} -1/(R_1 C_1) & 0 & 0 \\ 0 & -1/(R_2 C_2) & 0 \\ 0 & 0 & 0 \end{bmatrix} \mathbf{b}(t) + \begin{bmatrix} 1/C_1 \\ 1/C_2 \\ -\zeta/Q \end{bmatrix} I(t), \quad (13)$$

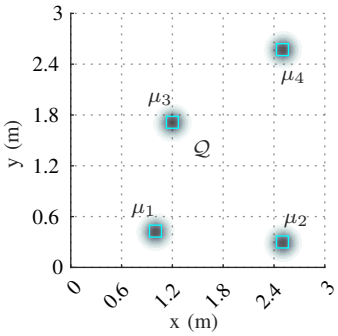

Fig. 3: **Information spatial distribution and search space** in our experimental evaluation. The distribution consists of four Gaussians in a Gaussian mixture model ϕ. The Gaussians are centered in μ_1, μ_2, μ_3, and μ_4, as depicted by the cyan empty squares. The search space $\mathcal{Q}$ is a three-by-three area. The resulting ergodic trajectories are expected to be such that the robot spends more time close to the Gaussians.

where $\zeta \in \mathbb{R}$ is a battery coefficient [29], $R_1, R_2 \in \mathbb{R}$ and $C_1, C_2 \in \mathbb{R}$ are resistors and capacitors relative to the first and second RC elements in the ECM measured in ohms and farads respectively. $Q \in \mathbb{R}$ is the battery nominal capacity measured in amperes per hour. $I \in \mathbb{R}$ is the internal current which is load-dependent, e.g., the current required to run the motors, actuators, etc. It is measured in amperes and assumed constant in flight from empirical observations of the aerial robot used in the experiments (see Sec. IV).

The state $\mathbf{b} := \begin{bmatrix} V_1 & V_2 & \mathbf{b}_{\text{SoC}} \end{bmatrix} \in \mathbb{R}^3$ contains three battery metrics. $V_1, V_2 \in \mathbb{R}$ are the voltages measured in volts across the first and second RC elements, and $\mathbf{b}_{\text{SoC}} \in (0, 1]$ is the normalized battery SoC that evolves from fully charged – or from a given initial value $\mathbf{b}_{\text{SoC}}(t_0)$ – to discharged. Battery voltage $V_e \in \mathbb{R}$ measured in volts can be expressed

$$V_e(t) = V\big(\mathbf{b}_{\text{SoC}}(t)\big) - V_1(t) - V_2(t) - I(t)R, \qquad (14)$$

where $R \in \mathbb{R}$ is the single resistor measured in ohms in Fig. 2, and V is the open circuit voltage that can be retrieved from the datasheet [38].

The values of R_1, C_1, R_2, C_2, R are identified so that the model output and the physical behavior of the agents are matched as closely as possible [32] (see Sec. IV).

The battery model can be used to derive the battery SoC and voltage in Eq. (13) and (14). The battery SoC depends on Q and ζ and is utilized to find the control action $\mathbf{u}(t)$ so that there is at least one agent exploring. The voltage depends on the two RC elements and is utilized to evaluate the SoC of a physical system, i.e., it can be compared to the battery voltage provided by a flight controller. When the solution of the OCP in Eq. (12) is evaluated, the battery model in Eq. (13) is integrated for the duration of the horizon. The recharging is approximated with the expression $\mathbf{b}_{\text{SoC}} = \eta\, \mathbf{b}_{\text{SoC}} + \theta$ for given $\eta, \theta \in \mathbb{R}$ determined empirically.

IV. Experimental Results

In this section, we discuss our experimental setup and results. Our experiments are implemented in simulation using MATLAB (R), and physical experiments are implemented in Python and conducted using Crazyflie 2.0 micro aerial vehicles (MAVs). The dynamics $\dot{\mathbf{q}} = f(\mathbf{q}, \mathbf{u})$ is that of a 2D single integrator system, which mimics the MAV control reasonably [14]. The chosen dynamics is not specific to our implementation. The physical setup is illustrated in Fig. 1.

The source code[1] is released under the non-commercial open-source license CC BY-NC-SA 4.0. The solution of the OCP in Eq. (12) relies on two external open-source components from the literature: the popular nonlinear programming solver IPOPT [40] and a software framework for nonlinear optimization called CasADi [41]. The simulation is derived offline first, but the computational load is not prohibitive, i.e., online runtime is possible (see Sec. V). Each MAV is equipped with a positioning and wireless charging decks. Precise positioning of MAVs is achieved via two HTC SteamVR Base Station 2.0 units. Each MAV is then equipped with a one-cell 250 mAh 3.7 volts LiPo battery.

We evaluate our approach under two different scenarios. In both scenarios, we use a three-by-three-meter space where the knowledge of the environment is assumed. The spatial distribution ϕ contains four Gaussians in the GMM in Eq. (2) in the second scenario, as illustrated in Fig. 3 (the four cyan empty squares). In the first scenario, it contains one Gaussian centered in μ_2 first, and it contains two Gaussians centered in μ_2 and μ_3 later.

Competing exploration

In the first scenario, four MAVs α_1, α_2, α_3, and α_4 are placed on top of four wireless charging stations. The horizon is set

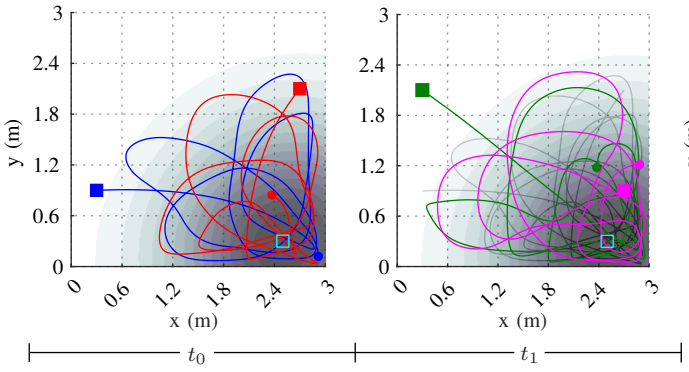

Fig. 4: **Experimental evaluation of competing exploration with one Gaussian**. Four agents α_1, α_2, α_3, and α_4 explore the space two-by-two first, and they compete for one area with high information density. The agents α_1 blue and α_2 red explore the space in the first horizon t_0 (left of the figure), spending most of the time close to the Gaussian. The agents then return to the charging station to recharge the battery. The other two agents α_3 dark green and α_4 magenta proceed in the next time horizon.

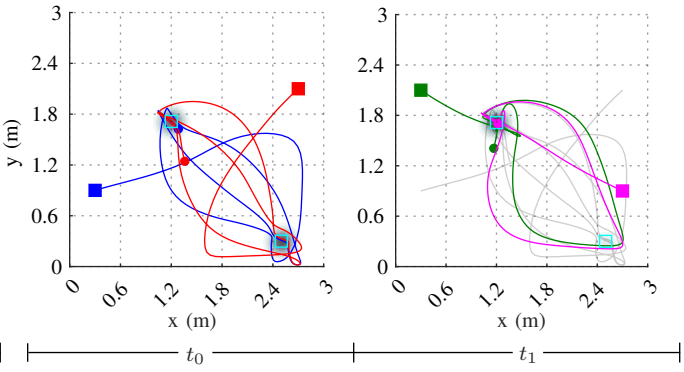

Fig. 5: **Experimental evaluation of competing exploration with two Gaussians**. Four agents explore the space and compete for two areas with high information density (instead of one in Fig. 4). The agents blue and red are selected first. One can note how both agents swap between the areas but spend most time near the Gaussians. At the end of the first horizon, they return to the charging stations with the other two agents dark green and magenta exploring the space.

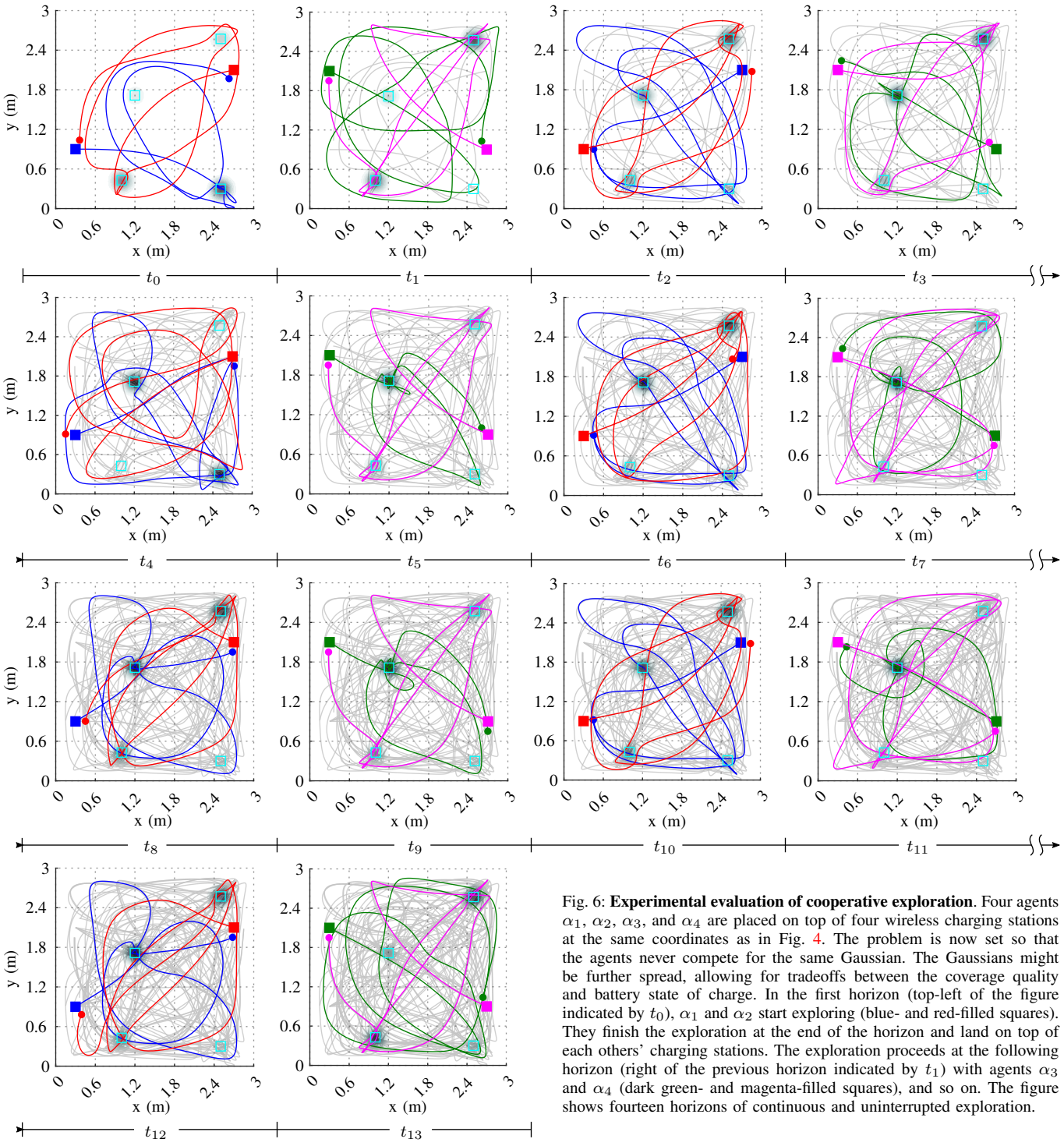

Fig. 6: **Experimental evaluation of cooperative exploration**. Four agents α_1, α_2, α_3, and α_4 are placed on top of four wireless charging stations at the same coordinates as in Fig. 4. The problem is now set so that the agents never compete for the same Gaussian. The Gaussians might be further spread, allowing for tradeoffs between the coverage quality and battery state of charge. In the first horizon (top-left of the figure indicated by t_0), α_1 and α_2 start exploring (blue- and red-filled squares). They finish the exploration at the end of the horizon and land on top of each others' charging stations. The exploration proceeds at the following horizon (right of the previous horizon indicated by t_1) with agents α_3 and α_4 (dark green- and magenta-filled squares), and so on. The figure shows fourteen horizons of continuous and uninterrupted exploration.

to two and a half minutes and is derived empirically along with battery and recharging coefficients. The battery values used in the scenario are scaled from [32]. The number of frequencies K is set to nine, as in [33]. The MAVs compete for the same area with high information density, i.e., they utilize the multi-agent ergodic metric introduced in Eq. (10). The battery constraint is edited so that there are two MAVs first, i.e.,

$$\exists_{=1}\, k_1, k_2 \in [n] \text{ s.t. } {}^{k_1}\mathbf{b}_{\text{SoC}}, {}^{k_2}\mathbf{b}_{\text{SoC}} \in (0, b_f], \tag{15}$$

where $\exists_{=1}$ indicates the unique existential quantification.

Initially, two MAVs are selected via the solution to the OCP in Eq. (12), α_1 "blue" and α_2 "red." They are located at coordinates $(0.3,0.9)$ and $(2.7,2.1)$ respectively, denoted by the blue and red filled squares in Fig. 4. The MAVs explore the space for the first horizon, focusing on the area with high information density. At the end of the horizon (blue and red filled dots), the MAVs return to the charging stations.

Once the two agents α_1 and α_2 land, they start recharging. The formulation of the OCP in Eq. (12) is such that the other two agents α_3 "dark green" and α_4 "magenta" are selected.

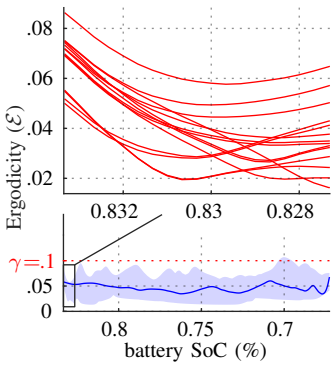

Fig. 7: **Ergodicity as a function of state-of-charge**. The top plot shows the evolution of the ergodicity for all the horizons in Fig. 6. The bottom shows the average ergodicity. Initially, the MAVs are at their charging stations. As they start exploring, they move to the areas with high information density – ergodicity decreases. As they approach the end of the horizon, they start moving to the charging stations – ergodicity increases. The average ergodicity can be observed to be under the value γ.

They are located at coordinates (0.3,2.1) and (2.7,0.9). In the following horizon, agents α_3 and α_4 are recharging whereas α_1 and α_2 proceed with the exploration, and so on.

Fig. 5 illustrates the case of the agents competing for two areas with high information density.

Cooperative exploration

In the second extensive scenario, four MAVs α_1, α_2, α_3, and α_4 are placed on top of four wireless charging stations, as in the previous scenario. The optional constraints in Eq. (12f) are built so that each MAV covers two Gaussians at a time that are respectively farthest (μ_3 and μ_2 are the centers of the Gaussians covered by the blue and dark green agents, μ_1 and μ_4 are the centers of the Gaussians covered by the red and magenta agents in Fig. 6). This means that the MAVs will never compete for the same Gaussian, but will cooperate in the exploration.

There is an additional constraint on the final point in Eq (12g), set so that the agents have to be in the proximity of a charging station. The actual constraint is derived in Eq. (17). The cost function in Eq. (12a) is further enhanced with the mixing coefficient $\boldsymbol{\delta}$ in Eq. (2), allowing us to find the tradeoffs between the single Gaussians, the different agents, and the battery SoC. Namely, the cost is

$$\min_{\boldsymbol{\Theta},\boldsymbol{\delta}} \ \frac{1}{n}\sum_{k=1}^{n}\int_{\mathcal{T}_k} {}^{k}\mathbf{u}(\tau)^T R_k\, {}^{k}\mathbf{u}(\tau)\, d\tau - \sum_{k=1}^{m}\delta_k. \tag{16}$$

A similar approach is undertaken in prior literature [16], where the ergodic objective is dynamic as more information is gathered, rather than the battery status is changed.

The number of frequencies, battery and recharging coefficients, and the horizon are those used in the previous scenario. The ergodic metric is set to be lower or equal to 0.1, in line with similar literature [14].

The results are shown in Fig. 6. The figure is to be read from left to right and from top to bottom, with the horizons being indicated under each subfigure (meaning that t_0 is the first horizon, t_1 is the second horizon, etc.). Initially, two MAVs are selected via the solution to the OCP in Eq. (12), α_1 blue and α_2 red, similarly to the previous scenario. The energy-aware ergodic trajectories ${}^{1}\mathbf{q}(t)$ and ${}^{2}\mathbf{q}(t)$ are selected so that the MAVs land at each other's charging stations, i.e., ${}^{1}\mathbf{q}(t_f) = {}^{2}\mathbf{q}(t_0)$ and vice-versa. The mixing coefficients for α_1 are such that $\delta_2 > \delta_3$, meaning that the agent α_1 explores in more detail the area delimited by the Gaussian centered in μ_2. This is indicated by the darker coloring of the different Gaussians, which is proportional to the optimal value of $\boldsymbol{\delta}$. An analogous situation is to be observed with agent α_2.

To guarantee that both agents land on top of each other's charging stations (the red and blue filled dots at the end of the trajectories for α_2 and α_1) respectively, the constraint in Eq. (12g) is evaluated within

$$\|{}^{k_2}\mathbf{q}(t_f) - {}^{k_1}\mathbf{q}(t_0)\| \leq \varepsilon, \tag{17}$$

where $\varepsilon \in \mathbb{R}_{>0}$ and $k_1, k_2 \in [n]$ are given.

Once the two agents α_1 and α_2 land, they start recharging. The other two agents α_3 dark green and α_4 magenta are selected. They proceed on the respective energy-aware ergodic trajectories and land on top of each other's charging stations, with the past trajectory being indicated in the background in gray. The figure shows fourteen horizons.

Ergodicity against battery state of charge

We report the evolution of the value of the ergodic metric in Eq. (3) in time as a function of the battery SoC in Fig. 7. The experimental data are from the cooperative exploration.

The top of the figure shows the evolution per each horizon in red, whereas the bottom shows the average value in blue. We can observe that the exploration starts at an initial value of ergodicity, which mostly depends on the distance from the charging stations to the components of the GMM (i.e., high information density). The ergodicity decreases as the agents move towards the Gaussians in the spatial distribution GMM. It oscillates as the agents move from one Gaussian to another. In the first half of the horizon, the average ergodicity continues to descend as more information is gathered. In the second, the ergodicity increases, peaking at the end, as the discharged agents return to the charging stations for recharging (i.e., low information density).

V. Conclusion and Future Directions

This work enhances prior literature on ergodic search and answers the question of whether is it possible to explore a space uninterruptedly, with at least one agent at all times. Our methods are to derive an abstract battery model and extend the canonical ergodic search – a method to derive robots' trajectories that visit areas with high information density – to energy-aware ergodic search. Continuous exploration is achieved using an optimization framework, which resembles a model predictive controller formulation. Experimental data indicate the effectiveness of our battery-constrained exploration. Continuous and uninterrupted coverage is achieved with a multi-agent system so that there is always at least one agent exploring and the spatial distribution is satisfied – a statement that we prove with empirical evidence.

A limitation of the current methods is that the charging stations are in fixed positions and the information is centralized. To enable real-world use cases, we are currently extending the methods to mobile charging stations and decentralized systems, which arise in scenarios such as environmental surveying. In future work, we are also planning to investigate other aspects, including energy optimality, online runtime, etc., which are currently not addressed.

References

[1] H. Choset, "Coverage for robotics–A survey of recent results," *Annals of Mathematics and Artificial Intelligence*, vol. 31, pp. 113–126, 2001. 1

[2] E. Galceran and M. Carreras, "A survey on coverage path planning for robotics," *Robotics and Autonomous Systems*, vol. 61, no. 12, pp. 1258–1276, 2013. 1

[3] T. M. Cabreira, L. B. Brisolara, and P. R. Ferreira Jr., "Survey on coverage path planning with unmanned aerial vehicles," *Drones*, vol. 3, no. 1, p. 38, 2019. 1

[4] I. Abraham, A. Prabhakar, and T. D. Murphey, "An ergodic measure for active learning from equilibrium," *IEEE Transactions on Automation Science and Engineering*, vol. 18, no. 3, pp. 917–931, 2021. 1, 2

[5] L. M. Miller, Y. Silverman, M. A. MacIver, and T. D. Murphey, "Ergodic exploration of distributed information," *IEEE Transactions on Robotics*, vol. 32, no. 1, pp. 36–52, 2016. 1, 2

[6] L. Dressel and M. J. Kochenderfer, "On the optimality of ergodic trajectories for information gathering tasks," in *IEEE American Control Conference (ACC)*, 2018, pp. 1855–1861. 1, 2

[7] G. De La Torre, K. Flaßkamp, A. Prabhakar, and T. D. Murphey, "Ergodic exploration with stochastic sensor dynamics," in *IEEE American Control Conference (ACC)*, 2016, pp. 2971–2976. 1, 2

[8] S. Shetty, J. Silvério, and S. Calinon, "Ergodic exploration using tensor train: Applications in insertion tasks," *IEEE Transactions on Robotics*, vol. 38, no. 2, pp. 906–921, 2022. 1, 2

[9] A. Prabhakar, I. Abraham, A. Taylor, M. Schlafly *et al.*, "Ergodic specifications for flexible swarm control: From user commands to persistent adaptation," in *Conference on Robotics: Science and Systems (RSS)*, 2020, p. 9. 1, 2

[10] H. Coffin, I. Abraham, G. Sartoretti, T. Dillstrom *et al.*, "Multi-agent dynamic ergodic search with low-information sensors," in *IEEE International Conference on Robotics and Automation (ICRA)*, 2022, pp. 11 480–11 486. 1, 2

[11] C. Lerch, D. Dong, and I. Abraham, "Safety-critical ergodic exploration in cluttered environments via control barrier functions," in *IEEE International Conference on Robotics and Automation (ICRA)*, 2023, pp. 10 205–10 211. 1, 2

[12] I. Abraham and T. D. Murphey, "Decentralized ergodic control: Distribution-driven sensing and exploration for multiagent systems," *IEEE Robotics and Automation Letters*, vol. 3, no. 4, pp. 2987–2994, 2018. 1, 2

[13] S. Patel, S. Hariharan, P. Dhulipala, M. C. Lin *et al.*, "Multi-agent ergodic coverage in urban environments," in *IEEE International Conference on Robotics and Automation (ICRA)*, 2021, pp. 8764–8771. 1, 2

[14] D. Dong, H. Berger, and I. Abraham, "Time optimal ergodic search," in *Conference on Robotics: Science and Systems (RSS)*, 2023, p. 13. 1, 3, 4, 6

[15] I. Abraham, A. Prabhakar, M. J. Z. Hartmann, and T. D. Murphey, "Ergodic exploration using binary sensing for nonparametric shape estimation," *IEEE Robotics and Automation Letters*, vol. 2, no. 2, pp. 827–834, 2017. 1

[16] A. Rao, A. Breitfeld, A. Candela, B. Jensen *et al.*, "Multi-objective ergodic search for dynamic information maps," in *IEEE International Conference on Robotics and Automation (ICRA)*, 2023, pp. 10 197–10 204. 1, 6

[17] E. Ayvali, H. Salman, and H. Choset, "Ergodic coverage in constrained environments using stochastic trajectory optimization," in *IEEE/RSJ International Conference on Intelligent Robots and Systems (IROS)*, 2017, pp. 5204–5210. 1, 3

[18] G. Mathew and I. Mezić, "Metrics for ergodicity and design of ergodic dynamics for multi-agent systems," *Physica D: Nonlinear Phenomena*, vol. 240, no. 4, pp. 432–442, 2011. 1, 2

[19] L. M. Miller and T. D. Murphey, "Trajectory optimization for continuous ergodic exploration," in *IEEE American Control Conference (ACC)*, 2013, pp. 4196–4201. 1, 2

[20] C. Di Franco and G. Buttazzo, "Energy-aware coverage path planning of UAVs," in *IEEE International Conference on Autonomous Robot Systems and Competitions (ICARSC)*, 2015, pp. 111–117. 1

[21] ——, "Coverage path planning for UAVs photogrammetry with energy and resolution constraints," *Journal of Intelligent & Robotic Systems*, vol. 83, no. 3, pp. 445–462, 2016. 1

[22] I. Shnaps and E. Rimon, "Online coverage of planar environments by a battery powered autonomous mobile robot," *IEEE Transactions on Automation Science and Engineering*, vol. 13, no. 2, pp. 425–436, 2016. 1

[23] T. M. Cabreira, C. D. Franco, P. R. Ferreira Jr., and G. C. Buttazzo, "Energy-aware spiral coverage path planning for UAV photogrammetric applications," *IEEE Robotics and Automation Letters*, vol. 3, no. 4, pp. 3662–3668, 2018. 1

[24] M. Wei and V. Isler, "Coverage path planning under the energy constraint," in *IEEE International Conference on Robotics and Automation (ICRA)*, 2018, pp. 368–373. 1

[25] K. R. Jensen-Nau, T. Hermans, and K. K. Leang, "Near-optimal area-coverage path planning of energy-constrained aerial robots with application in autonomous environmental monitoring," *IEEE Transactions on Automation Science and Engineering*, vol. 18, no. 3, pp. 1453–1468, 2021. 1

[26] Y. Mei, Y.-H. Lu, Y. C. Hu, and C. G. Lee, "Energy-efficient motion planning for mobile robots," in *IEEE International Conference on Robotics and Automation (ICRA)*, vol. 5, 2004, pp. 4344–4349. 1

[27] ——, "A case study of mobile robot's energy consumption and conservation techniques," in *IEEE International Conference on Advanced Robotics (ICAR)*, 2005, pp. 492–497. 1

[28] C. H. Kim and B. K. Kim, "Energy-saving 3-step velocity control algorithm for battery-powered wheeled mobile robots," in *IEEE International Conference on Robotics and Automation (ICRA)*, 2005, pp. 2375–2380. 1

[29] A. Seewald, H. García de Marina, H. S. Midtiby, and U. P. Schultz, "Energy-aware planning-scheduling for autonomous aerial robots," in *IEEE/RSJ International Conference on Intelligent Robots and Systems (IROS)*, 2022, pp. 2946–2953. 1, 3, 4

[30] P. Ondrúška, C. Gurău, L. Marchegiani, C. H. Tong *et al.*, "Scheduled perception for energy-efficient path following," in *IEEE International Conference on Robotics and Automation (ICRA)*, 2015, pp. 4799–4806. 1

[31] S. Sudhakar, S. Karaman, and V. Sze, "Balancing actuation and computing energy in motion planning," in *IEEE International Conference on Robotics and Automation (ICRA)*, 2020, pp. 4259–4265. 1

[32] S. Zhao, S. R. Duncan, and D. A. Howey, "Observability analysis and state estimation of lithium-ion batteries in the presence of sensor biases," *IEEE Transactions on Control Systems Technology*, vol. 25, no. 1, pp. 326–333, 2017. 1, 3, 4, 5

[33] S. Calinon, *Mixture models for the analysis, edition, and synthesis of continuous time series*. Springer, 2020, pp. 39–57. 2, 3, 5

[34] A. Seewald, "Energy-aware coverage planning and scheduling for autonomous aerial robots," Ph.D. thesis, Syddansk Universitet, 2021, doi.org/10.21996/7ka6-r457. 3

[35] C. Zhang, W. Allafi, Q. Dinh, P. Ascencio *et al.*, "Online estimation of battery equivalent circuit model parameters and state of charge using decoupled least squares technique," *Energy*, vol. 142, pp. 678–688, 2018. 3

[36] X. Hu, S. Li, and H. Peng, "A comparative study of equivalent circuit models for Li-ion batteries," *Journal of Power Sources*, vol. 198, pp. 359–367, 2012. 3

[37] A. Hasan, M. Skriver, and T. A. Johansen, "eXogenous Kalman filter for state-of-charge estimation in lithium-ion batteries," in *IEEE Conference on Control Technology and Applications (CCTA)*, 2018, pp. 1403–1408. 3

[38] H. Hinz, "Comparison of lithium-ion battery models for simulating storage systems in distributed power generation," *Inventions*, vol. 4, p. 22, 2019. 3, 4

[39] S. Mousavi G. and M. Nikdel, "Various battery models for various simulation studies and applications," *Renewable and Sustainable Energy Reviews*, vol. 32, pp. 477–485, 2014. 3

[40] A. Wächter and L. T. Biegler, "On the implementation of an interior-point filter line-search algorithm for large-scale nonlinear programming," *Mathematical Programming*, vol. 106, no. 1, pp. 25–57, 2006. 4

[41] J. Andersson, J. Åkesson, and M. Diehl, "CasADi: A symbolic package for automatic differentiation and optimal control," in *Conference on Recent Advances in Algorithmic Differentiation (AD)*. Springer, 2012, pp. 297–307. 4